SEARCH FOR MASSIVE RARE PARTICLES WITH MACRO

The MACRO Collaboration

M. Ambrosio[12], R. Antolini[7], G. Auriemma[14,a], D. Bakari[2,17], A. Baldini[13], G. C. Barbarino[12], B. C. Barish[4], G. Battistoni[6,b], R. Bellotti[1], C. Bemporad[13], P. Bernardini[10], H. Bilokon[6], V. Bisi[16], C. Bloise[6], C. Bower[8], M. Brigida[1], S. Bussino[18], F. Cafagna[1], M. Calicchio[1], D. Campana[12], M. Carboni[6], S. Cecchini[2,c], F. Cei[13], V. Chiarella[6], B. C. Choudhary[4], S. Coutu[11,l], G. De Cataldo[1], H. Dekhissi[2,17], C. De Marzo[1], I. De Mitri[10], J. Derkaoui[2,17], M. De Vincenzi[18], A. Di Credico[7], O. Erriquez[1], C. Favuzzi[1], C. Forti[6], P. Fusco[1], G. Giacomelli[2], G. Giannini[13,e], N. Giglietto[1], M. Giorgini[2], M. Grassi[13], L. Gray[7], A. Grillo[7], F. Guarino[12], C. Gustavino[7], A. Habig[3], K. Hanson[11], R. Heinz[8], E. Iarocci[6,f], E. Katsavounidis[4], I. Katsavounidis[4], E. Kearns[3], H. Kim[4], S. Kyriazopoulou[4], E. Lamanna[14,m], C. Lane[5], D. S. Levin[11], P. Lipari[14], N. P. Longley[4,i], M. J. Longo[11], F. Loparco[1], F. Maaroufi[2,17], G. Mancarella[10], G. Mandrioli[2], S. Manzoor[2,p], A. Margiotta[2], A. Marini[6], D. Martello[10], A. Marzari-Chiesa[16], M. N. Mazziotta[1], D. G. Michael[4], S. Mikheyev[4,7,g], L. Miller[8,n], P. Monacelli[9], T. Montaruli[1], M. Monteno[16], S. Mufson[8], J. Musser[8], D. Nicolò[13,d], R. Nolty[4], C. Okada[3], C. Orth[3], G. Osteria[12], M. Ouchrif[2,17], O. Palamara[7], V. Patera[6,f], L. Patrizii[2], R. Pazzi[13], C. W. Peck[4], L. Perrone[10], S. Petrera[9], P. Pistilli[18], V. Popa[2,h], A. Rainò[1], J. Reynoldson[7], F. Ronga[6], A. Rrhioua[2,17], C. Satriano[14,a], L. Satta[6,f], E. Scapparone[7], K. Scholberg[3], A. Sciubba[6,f], P. Serra[2], M. Sioli[2], G. Sirri[2], M. Sitta[16], P. Spinelli[1], M. Spinetti[6], M. Spurio[2], R. Steinberg[5], J. L. Stone[3], L. R. Sulak[3], A. Surdo[10], G. Tarlè [11], V. Togo[2], M. Vakili[15], E. Vilela[2], C. W. Walter[3,4] and R. Webb[15].

1. Dipartimento di Fisica dell'Università di Bari and INFN, 70126 Bari, Italy
2. Dipartimento di Fisica dell'Università di Bologna and INFN, 40126 Bologna, Italy
3. Physics Department, Boston University, Boston, MA 02215, USA
4. California Institute of Technology, Pasadena, CA 91125, USA
5. Department of Physics, Drexel University, Philadelphia, PA 19104, USA
6. Laboratori Nazionali di Frascati dell'INFN, 00044 Frascati (Roma), Italy

7. Laboratori Nazionali del Gran Sasso dell'INFN, 67010 Assergi (L'Aquila), Italy
8. Depts. of Physics and of Astronomy, Indiana University, Bloomington, IN 47405, USA
9. Dipartimento di Fisica dell'Università dell'Aquila and INFN, 67100 L'Aquila, Italy
10. Dipartimento di Fisica dell'Università di Lecce and INFN, 73100 Lecce, Italy
11. Department of Physics, University of Michigan, Ann Arbor, MI 48109, USA
12. Dipartimento di Fisica dell'Università di Napoli and INFN, 80125 Napoli, Italy
13. Dipartimento di Fisica dell'Università di Pisa and INFN, 56010 Pisa, Italy
14. Dipartimento di Fisica dell'Università di Roma "La Sapienza" and INFN, 00185 Roma, Italy
15. Physics Department, Texas A&M University, College Station, TX 77843, USA
16. Dipartimento di Fisica Sperimentale dell'Università di Torino and INFN, 10125 Torino, Italy
17. L.P.T.P., Faculty of Sciences, University Mohamed I, B.P. 524 Oujda, Morocco
18. Dipartimento di Fisica dell'Università di Roma Tre and INFN Sezione Roma Tre, 00146 Roma, Italy
a Also Università della Basilicata, 85100 Potenza, Italy
b Also INFN Milano, 20133 Milano, Italy
c Also Istituto TESRE/CNR, 40129 Bologna, Italy
d Also Scuola Normale Superiore di Pisa, 56010 Pisa, Italy
e Also Università di Trieste and INFN, 34100 Trieste, Italy
f Also Dipartimento di Energetica, Università di Roma, 00185 Roma, Italy
g Also Institute for Nuclear Research, Russian Academy of Science, 117312 Moscow, Russia
h Also Institute for Space Sciences, 76900 Bucharest, Romania
i The Colorado College, Colorado Springs, CO 80903, USA
l Also Department of Physics, Pennsylvania State University, University Park, PA 16801, USA
m Also Dipartimento di Fisica dell'Università della Calabria, Rende (Cosenza), Italy
n Also Department of Physics, James Madison University, Harrisonburg, VA 22807, USA
p Also RPD, PINSTECH, P.O. Nilore, Islamabad, Pakistan

Abstract

Massive rare particles have been searched for in the penetrating cosmic radiation using the MACRO apparatus at the Gran Sasso National Laboratories. Liquid scintillators, streamer tubes and nuclear track detectors have been used to search for magnetic monopoles (MMs). Based on no observation of such signals, stringent flux limits are established for MMs as slow as a few $10^{-5}c$.

The methods based on the scintillator and on the nuclear track subdetectors were also applied to search for nuclearites.

Preliminary results of the searches for charged Q-balls are also presented.

1 INTRODUCTION

One of the primary aims of the MACRO experiment at the Gran Sasso underground Laboratories is the search for magnetic monopoles at the mass scale of Grand Unified Theories (GUTs) of the electroweak and strong interactions [1] with a sensitivity well below the Parker bound (10^{-15} cm^{-2} s^{-1} sr^{-1}) [2] in the velocity range $4 \cdot 10^{-5} < \beta < 1$, $\beta = v/c$.

MACRO has three subdetectors: liquid scintillation counters, limited streamer tubes and nuclear track detectors (CR39 and Lexan) arranged in a modular structure of six "supermodules" (SM's). Each SM is divided into a lower and an upper ("Attico") part and comes with separate mechanical structure and electronics readout. The full detector has global dimensions of $76.5 \times 12 \times 9.3$ m^3 [3] and provides a total acceptance to an isotropic flux of particles of $\sim 10,000$ m^{2}sr. The detector has been built and equipped with electronics during the years 1988-1995. Data taking began in 1989 with the first SM; since the fall of 1995 it is running in its final configuration. The response to slow and fast particles of the scintillators, streamer tubes and nuclear track detectors was experimentally studied [4, 5, 6]. The three subdetectors ensure redundancy of information, cross-checks and independent signatures for possible MM candidates.

The analyses presented here, based on the various subdetectors in a stand-alone and in a combined way, refer to direct detection of bare MMs of one unit Dirac charge ($g_D = 137/2e$), catalysis cross section $\sigma_{cat} < 1$ mb and isotropic flux (we consider MMs with enough kinetic energy to traverse the Earth); this last condition sets a β dependent mass threshold ($\sim 10^{17}$ GeV for $\beta \sim 5 \cdot 10^{-5}$, and lower for faster MMs). Since no MM candidate was found we quote new flux upper limits at the level of $2.5 \cdot 10^{-16}$ cm^{-2} s^{-1} sr^{-1} for $\beta > 5 \cdot 10^{-5}$.

"Strange Quark Matter" (SQM) should consist of aggregates of comparable amounts of u, d and s quarks; it might be the ground state of QCD [7]. If bags of SQM were produced in a first-order phase transition in the early universe, they could be candidates for the Dark Matter (DM), and might be found in the cosmic radiation reaching the Earth. SQM in the cosmic radiation is commonly known as "nuclearite" and "strangelet"[8].

Q-balls should be aggregates of squarks, sleptons and Higgs fields [9, 10]. They could have been produced in the early Universe, and may contribute to the Cold Dark Matter. Heavy Q-balls may have originated in the course of a phase transition or they could have been produced via fusion processes, reminiscent of the big bang nucleosynthesis. Small Q-balls could also be

pair-produced in very high energy collisions. Relic Q-balls can be separated in two classes: Supersymmetric Electrically Charged Solitons (SECS) and Supersymmetric Electrically Neutral Solitons (SENS).

Some of the methods used for the MM searches may also be applied to search for nuclearites and for charged Q-balls (SECS). We quote upper limits for $\beta > 5 \cdot 10^{-5}$.

2 SEARCHES FOR MAGNETIC MONOPOLES

A flux of cosmic GUT supermassive magnetic monopoles may reach the Earth. The velocity spectrum of these MMs could be in the range $4 \cdot 10^{-5} < \beta < 0.1$. Our searches for MMs exploit their energy loss mechanisms in each of the three MACRO subdetectors.

In scintillators the fraction of energy loss which is effective for the detection is the excitation energy loss which leads to the emission of light; in streamer tubes it is the ionization energy loss in the gas; in nuclear track detectors it is the Restricted Energy Loss (REL), i. e., the energy deposited within ~ 10 nm from the MM trajectory. In Ref. [11] a thorough analysis is made of these losses and of their dependence on the MM velocity.

Independent and combined monopole analyses were performed using the scintillator, streamer tube and nuclear track subdetectors in different ranges of velocity. As already stated the results presented here apply to bare g_D MMs and $\sigma_{cat} < 1$ mb; for the streamer tube analysis the dependence of the results on σ_{cat} is discussed below.

2.1 Searches with scintillators

The searches with the liquid scintillator subdetector use different specialized triggers covering specific velocity regions; the searches are grouped into searches for low velocity ($10^{-4} < \beta < 10^{-3}$), medium velocity ($10^{-3} < \beta < 10^{-1}$) and high velocity ($\beta > 0.1$) particles.

2.1.1 Low velocity monopole searches

Previous searches using data collected with the Slow Monopole Trigger (SMT) and Waveform Digitizer (WFD) were reported in Ref. [12], see curves "A", "B" in Fig. 1. A new custom made 200 MHz WFD system was implemented in 1995 which improves by at least a factor of two the sensitivity to very slow monopoles ($\beta \sim 10^{-4}$) and by over a factor of five

the sensitivity to relativistic monopoles with respect to previous conditions. The sensitivity of the SMT/WFD was tested with LED pulses, of ~ 6.3 μs duration, corresponding to $\beta \sim 10^{-4}$, down to the level of few tens of single photoelectrons, which is the signature of a slow monopole. A waveform analysis procedure consisted in scanning off-line the corresponding wave forms and in software simulation of the function of both the analog and digital part of the SMT circuitry on an event-by-event basis. We plan to report on this search in the near future.

2.1.2 Medium and high velocity monopole searches

The data collected by the PHRASE (Pulse Height Recorder and Synchronous Encoder) trigger are used to search for MMs in the range $1.2 \cdot 10^{-3} < \beta < 10^{-1}$ [12, 13]. The events are selected requiring hits in a maximum of four adjacent scintillation counters, with a minimum energy deposition of 10 MeV in two different scintillator layers. Events with $1.2 \cdot 10^{-3} < \beta < 5 \cdot 10^{-3}$ are rejected because their pulse width is smaller than the expected counter crossing time; events with $5 \cdot 10^{-3} < \beta < 10^{-1}$ are rejected because the light produced is much lower than that expected for a MM. The analyses refer to data collected by the MACRO lower part from October 1989 to the end of 1999 and also by the Attico from June 1995 to the end of 1999. No candidate survives; the 90% C.L. flux upper limit is $2.6 \cdot 10^{-16}$ cm^{-2} s^{-1} sr^{-1} (curve "D" in Fig. 1).

A previous search for MMs with $\beta > 10^{-1}$ based on the ERP (Energy Reconstruction Processor) trigger [12, 13] is included in Fig. 1 (curve "C").

2.2 Search using the streamer tubes

The streamer tube search was described in Refs. [12, 14]. The detection of MMs of $10^{-4} < \beta < 10^{-3}$ is based on the Drell and Penning effects in the gas mixture (73% He and 27% n-pentane) filling the tubes [14, 15]. The analysis is based on the search for single tracks in the streamer tubes and on the measurement of the velocity with the "time track". Only the horizontal streamer planes of the lower MACRO structure are used in the trigger; the Attico and the vertical planes are used for event reconstruction. Data were collected from January 1992 to end of 1999 for a live-time of $6.6 \cdot 10^4$ hours. The trigger and the analysis chain were checked to be velocity independent. The global efficiency was estimated by computing the ratio of the rate of single muons reconstructed by this analysis to the expected one [14]. The

overall efficiency was 74%. The detector acceptance, computed by a Monte Carlo simulation including geometrical and trigger requirements, is 4250 m^2 sr . No monopole candidate was found. For $1.1 \cdot 10^{-4} < \beta < 5 \cdot 10^{-3}$ the flux upper limit is $3.1 \cdot 10^{-16}$ cm^{-2} s^{-1} sr^{-1} at 90% C.L. (Fig. 1, curve "Streamer").

2.2.1 Catalysis of nucleon decay

Detailed Monte Carlo simulations were performed to study the effects of nucleon decay catalyzed by a GUT magnetic monopole on the streamer monopole trigger and its effects on the relative analysis. Both the physical process and the detector response were introduced in the code, taking into account the theoretical predictions on the cross section and on the decay channels.

Many samples (each of 10,000 monopole events) were generated with constant monopole velocity $\beta = 10^{-4}$, $5 \cdot 10^{-3}$, 10^{-3}, $5 \cdot 10^{-2}$ and 10^{-2}, and with catalysis cross sections $\sigma_{cat} = 10^{-26}$, 10^{-25}, $5 \cdot 10^{-25}$ and 10^{-24} cm^2 (in the last two cases other samples with $\beta = 2 \cdot 10^{-4}$ and $2 \cdot 10^{-3}$ were produced); also a sample with no catalysis was simulated as a term of reference. These simulations were performed according to two different theoretical models for the catalysis cross section, one which considers it to have the same β dependence for both protons and neutrons and a second one which assumes it to be β–enhanced in case of protons.

All samples were analyzed with the same program used for the real data. This allowed a study of the detection efficiency as a function of β and σ_{cat}. As a consequence new upper limits can be established which take into account also this process. Figs. 2 and 3 show for a catalysis event with $\beta = 10^{-3}$ and $\sigma_{cat} = 10^{-25}$ cm^2 the time and wire views, respectively: in the time view the monopole straight track and the catalysis hits are clearly distinguishable. Fig. 4 shows the distributions of the reconstructed β: the distributions are exactly peaked on the input values, which means that the reconstruction code works well also in the presence of catalysis hits. Finally Fig. 5 shows the upper limits vs β for different σ_{cat}: for low catalysis cross sections ($\sigma_{cat} \leq 10^{-25}$ cm^2) the difference is negligible, while for higher values it becomes more important.

A new analysis is in progress searching for catalysis events in the real data. Moreover checks are being carried out to see how the catalysis may affect the combined fast monopole analysis (Sect. 2.4).

2.3 Search using the nuclear track subdetector

The nuclear track subdetector covers a surface of 1263 m^2 and the acceptance for fast MMs is 7100 m^2 sr. The subdetector is used as a stand-alone detector and in a "triggered mode" by the scintillator and streamer tube systems. A detailed description of the method of searching for MMs is given in Ref. [16]. On May 2000 we began the massive etching of the CR39 sheets using the Bologna and Gran Sasso facilities, at the rate of about 40 m^2/month. An area of 368 m^2 of CR39 has been analysed, with an average exposure time of 8.5 years. No candidate was found; the 90% C.L. upper limits on the MM flux are at the level of $3.7 \cdot 10^{-16}$ cm^{-2} s^{-1} sr^{-1} at $\beta \sim 1$, and $5.4 \cdot 10^{-16}$ cm^{-2} s^{-1} sr^{-1} at $\beta \sim 10^{-4}$ (Fig. 1, curves "CR39").

2.4 Combined searches for fast monopoles

A search for fast MMs with scintillator or streamer tubes is affected by the background due to energetic muons with large energy losses (the nuclear track detector is not affected). Two analyses, which combine the use of the three subdetector systems, were performed in order to achieve the highest rejection imposing looser requirements.

2.4.1 Streamer tubes+ERP

The analysis procedure is based on the scintillator and streamer tube data; the nuclear track detector is used as a final tool for rejection/confirmation of the selected candidates. The trigger requires at least one fired scintillation counter and 7 hits in the horizontal streamer planes. Candidates are selected on the basis of the scintillator light yield and of the digital (tracking) and analog (pulse charge) information from the streamer tubes. A further selection is then applied on the streamer tube pulse charge. After corrections for gain variations, geometrical and electronic non-linear effects [17], a 90% efficiency cut is applied on the average streamer charge. Possible candidates (~ 2/year) are analysed in the corresponding nuclear track detector modules. The analysis refers to about 36,980 live hours with an average efficiency of 77%. The geometrical acceptance, computed by Monte Carlo methods, including the analysis requirements, is 3565 m^2 sr. No candidate survives; the 90% C.L. flux upper limit is $6.3 \cdot 10^{-16}$ cm^{-2} s^{-1} sr^{-1} for MMs with $5 \cdot 10^{-3} < \beta < 0.99$ (curve "E" in Fig. 1).

2.4.2 PHRASE+Streamer tubes

MMs with $\beta > 10^{-2}$ are searched for by combining the streamer tube and PHRASE triggers. Streamer tubes are used to reconstruct the trajectory and pathlength, scintillators are used to measure the velocity and the light yield. Selected events ($\sim$ 50/year) have a single track and an energy deposition $>$ 200 MeV in three scintillator layers. The event energy loss is compared to that expected for a monopole with the same velocity. The analysis refers to about 8528 live hours from May, 1997 to June, 1998. No candidate survives. The geometrical acceptance, including analysis cuts, is 3800 m^2 sr. The 90% C.L flux upper limit is $2.3 \cdot 10^{-15}$ cm^{-2} s^{-1} sr^{-1} (curve "F" in Fig. 1).

3 SEARCHES FOR NUCLEARITES

The main energy loss mechanism for nuclearites passing through matter is elastic or quasi-elastic collisions [8]:

$$\frac{dE}{dx} = \sigma \rho v^2$$

where σ is the nuclearite cross section, v its velocity and ρ the mass density of the traversed medium.

For nuclearites with masses $M \geq 8.4 \cdot 10^{14}$ GeV ($\simeq$ 1.5 ng) the cross section may be approximated as:

$$\sigma \simeq \pi \cdot \left(\frac{3M}{4\pi\rho_N} \right)^{3/2}$$

where ρ_N (the density of SQM) is estimated to be $\rho_N \simeq 3.5 \cdot 10^{14}$ g/cm^3 [18]. For lighter nuclearites the collisions are governed by their electronic clouds, yielding $\sigma \simeq \pi \cdot 10^{-16}$ cm^2.

Assuming galactic velocities, $\beta \simeq 2 \cdot 10^{-3}$, nuclearites with masses $\leq 5 \cdot 10^{11}$ GeV cannot reach the detector; for $5 \cdot 10^{12} \leq M \leq 10^{21}$ GeV only downward going nuclearites can reach it; for $M > 10^{22}$ GeV nuclearites can reach MACRO from all directions. Scintillators are sensitive to the blackbody radiation emitted along the heated nuclearite paths down to $\beta \simeq 5 \cdot 10^{-5}$. The CR39 is sensitive to nuclearites down to $\beta \sim 10^{-5}$ [19]. The density of the gas mixture in the streamer tubes is too low to produce energy losses yielding ionization, so the streamer tubes are not useful for nuclearite searches.

Individual flux limits for nuclearites from the scintillator and CR39 subdetectors are presented in Fig. 6; curves "a - d" refer to earlier searches with scintillators [19]; curves "e" and "f" are the updated limits obtained using the PHRASE system (Sect. 2.1.2) and CR39 nuclear track detectors, respectively.

4 SEARCHES FOR CHARGED Q-BALLS

The detection of Q-balls in MACRO is discussed in Ref. [20]. In that work it is assumed that the main contribution to the energy losses of SECS passing through matter with velocities in the range $10^{-4} < \beta < 10^{-2}$ are due to the interaction of the SECS positive charge with the nuclei (nuclear contribution) and with the electrons (electronic contribution) of the traversed medium. Other energy loss mechanisms, like nuclearite energy loss, could be considered and are under investigation.

The MACRO subdetectors are sensitive to SECS for any value of the electric charge $Z_Q \geq 1$. The observational signatures of SECS are characterized by substantial energy release along a straight track with no attenuation throughout the detector [10]. The energy losses of SECS in different subdetectors are given in Ref. [20]. CR39 and scintillators are sensitive to Q-balls with $Z_Q \geq 1$ for $3 \cdot 10^{-5} \leq \beta \leq 0.1$ and $\beta \geq 6 \cdot 10^{-5}$, respectively; in streamer tubes the detection threshold is at $\beta = 2 \cdot 10^{-3}$. We checked that the methods to search for MMs based on the PHRASE system (Sect. 2.1.2), on the streamer tube system (Sect. 2.2) and on the nuclear track detector (Sect. 2.3) can be applied to SECS. Flux limits for Q-balls with $Z_Q \geq 1$ obtained with the MACRO scintillators (curves "PHRASE") and with streamer tubes (curve "Streamer") are shown in Fig. 7; the limit obtained with CR39 (curve "CR39" in Fig. 7) applies to Q-balls with $Z_Q = 1$.

5 CONCLUSIONS

No MM, no nuclearite, no Q-ball candidates were found in any of these searches.

The 90% C.L. flux limits for MMs versus β are shown in Fig. 1. The global MACRO limit is computed as $2.3/X_{total}$ where $X_{total} = \sum_i X'_i$, and the X'_i are the independent time integrated acceptances of different analyses. This limit is compared in Fig. 8 with the limits of other experiments which searched for bare MMs with $g = g_D$ and $\sigma_{cat} < 1$ mb [21-28].

Following the same procedure used for MMs, we obtain the 90% C.L. global MACRO limit for an isotropic flux of nuclearites (with masses $> 6{\cdot}10^{22}$ GeV/c^2, Fig. 6); at $\beta = 2{\cdot}10^{-3}$ the limit is $2.1{\cdot}10^{-16}$ cm^{-2} s^{-1} sr^{-1}. The MACRO limit for a flux of downgoing nuclearites is compared in Fig. 9 with the limits of other experiments [25,29-31]. The Galactic Dark Matter (DM) limit in Fig. 9 was estimated assuming that $\Phi_{max} = \rho_{DM} v/(2\pi M)$, where $\rho_{DM} \simeq 10^{-24}$ g/cm^3 is the local DM density, and M and v are the mass and the velocity of nuclearites, respectively.

There is a close connection between searches for Q-balls (type SECS), nuclearites and magnetic monopoles. The liquid scintillators, the limited streamer tubes and the nuclear track detector CR39 are sensitive to SECS. The limits for MMs obtained with the scintillators using the PHRASE system and with streamer tubes can be applied to SECS. The global MACRO limit for SECS with electric charge $Z_Q = 1$ is obtained following the same procedure as for MMs and nuclearites and is shown in Fig. 7 (curve "MACRO").

Acknowledgements.

We gratefully acknowledge the support of the director and of the staff of the Laboratori Nazionali del Gran Sasso and the invaluable assistance of the technical staff of the Institutions participating in the experiment. We thank the Istituto Nazionale di Fisica Nucleare (INFN), the U.S. Department of Energy and the U.S. National Science Foundation for their generous support of the MACRO experiment. We thank INFN, ICTP (Trieste) and World Laboratory for providing fellowships and grants for non Italian citizens.

References

[1] J.Preskill, Phys. Rev. Lett. 43 (1979) 1365.

[2] M. S. Turner, E. M. Parker and T. J. Bogdan, Phys. Rev. D26 (1982) 1926.

[3] S. P. Ahlen et al., MACRO Coll., Nucl. Instr. & Meth. A324 (1993) 337.

[4] S. P. Ahlen and G. Tarlé, Phys. Rev. D27 (1983) 688; G. Giacomelli et al., hep-ex/0005041 (2000).

[5] G. Battistoni et al., Nucl. Instr. & Meth. A270 (1988) 185; G. Battistoni et al., Nucl. Instr. & Meth. A401 (1997) 309.
[6] S. Cecchini et al., Nuovo. Cim. A109 (1996) 1119.
[7] E. Witten, Phys. Rev. D30 (1984) 272.
[8] A. De Rújula and S. L. Glashow, Nature 312 (1984) 734.
[9] S. Coleman, Nucl. Phys. B262 (1985) 293.
[10] A. Kusenko, Phys. Lett. B404 (1997) 285; Phys. Lett. B405 (1997) 108; A. Kusenko and M. Shaposhnikov, Phys. Lett. B417 (1998) 99.
[11] J. Derkaoui et al., Astrop. Phys. 10 (1999) 339.
[12] M. Ambrosio et al., MACRO Coll., Phys. Lett. B406 (1997) 249.
[13] M. Ambrosio et al., MACRO Coll., Astropart. Phys. 1 (1992) 11.
[14] M. Ambrosio et al., MACRO Coll., Astrop. Phys.4 (1995) 33.
[15] S. Drell et al., Phys. Rev. Lett. 50 (1983) 644.
[16] M. Giorgini for the MACRO Coll., Nucl. Phys. B (Proc. Suppl) 85 (2000) 227.
[17] G. Battistoni et al., Nucl. Instr. & Meth. A399 (1997) 244.
[18] S. Chin and A. Kerman, Phys. Rev. Lett. 43 (1971) 1292.
[19] M. Ambrosio et al., MACRO Coll., hep-ex/9904031, Eur. Phys. J. C 13 (2000) 453.
[20] D. Bakari et al., hep-ex/0003003, Astrop. Phys. (in press) (2000).
[21] S. Bermon et al., Phys. Rev. Lett. 64 (1990) 839.
[22] K.N. Buckland et al., Phys. Rev. D41 (1990) 2726.
[23] J. L. Thron et al., Phys. Rev. D46 (1992) 4846.
[24] E. N. Alexeyev et al., 21^{st} ICRC, Adelaide, vol. 10 (1990) 83.
[25] S. Orito et al., Phys. Rev. Lett. 66 (1991) 1951.
[26] H. Adarkar et al., 21^{st} ICRC, Adelaide, vol. 10 (1990) 95.
[27] T. Hara et al., 21^{st} ICRC, Adelaide, vol. 10 (1990) 79.
[28] G. Domogatsky for the Baikal Coll. Talk presented at the XIX Int. Conf. on Neutrino Physics and Astrophysics, Sudbury, Canada (2000).
[29] S. Nakamura et al., Phys. Lett. B 263 (1991) 529.
[30] P. B. Price, Phys. Rev. D 38 (1988) 3813.
[31] D. Ghosh and S. Chatterjea, Europhys. Lett. 12 (1990) 25.

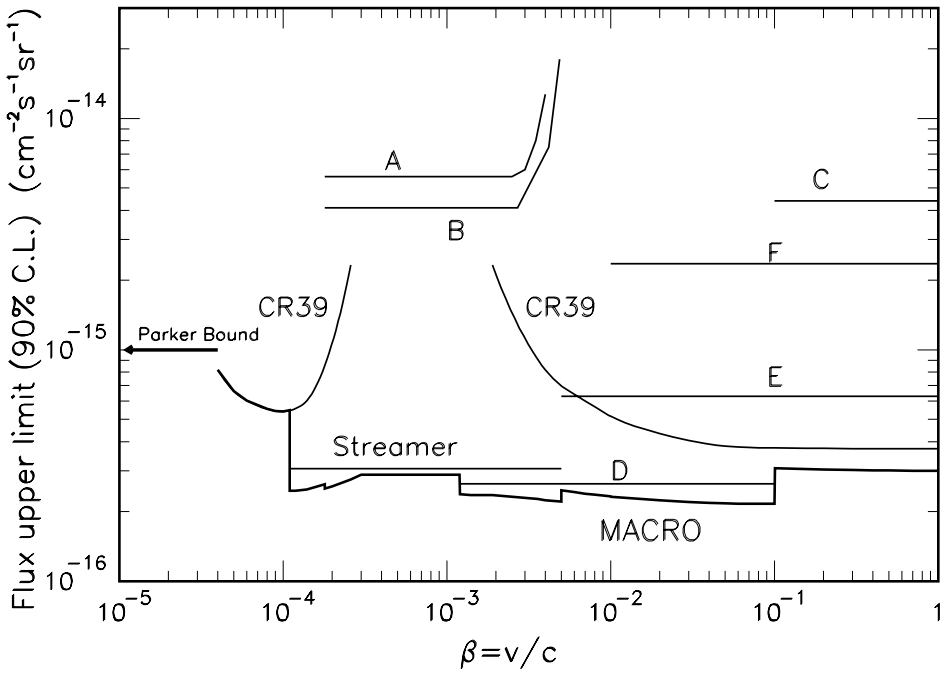

Figure 1: The 90% C.L. upper limits for an isotropic flux of supermassive magnetic monopoles obtained using the three MACRO subdetectors: liquid scintillators (curves A-D), streamer tubes (curve " Streamer"), nuclear track detectors (curves "CR39"); curves E and F were obtained combining the three subdetectors together (see text). The bold line is the present MACRO global limit.

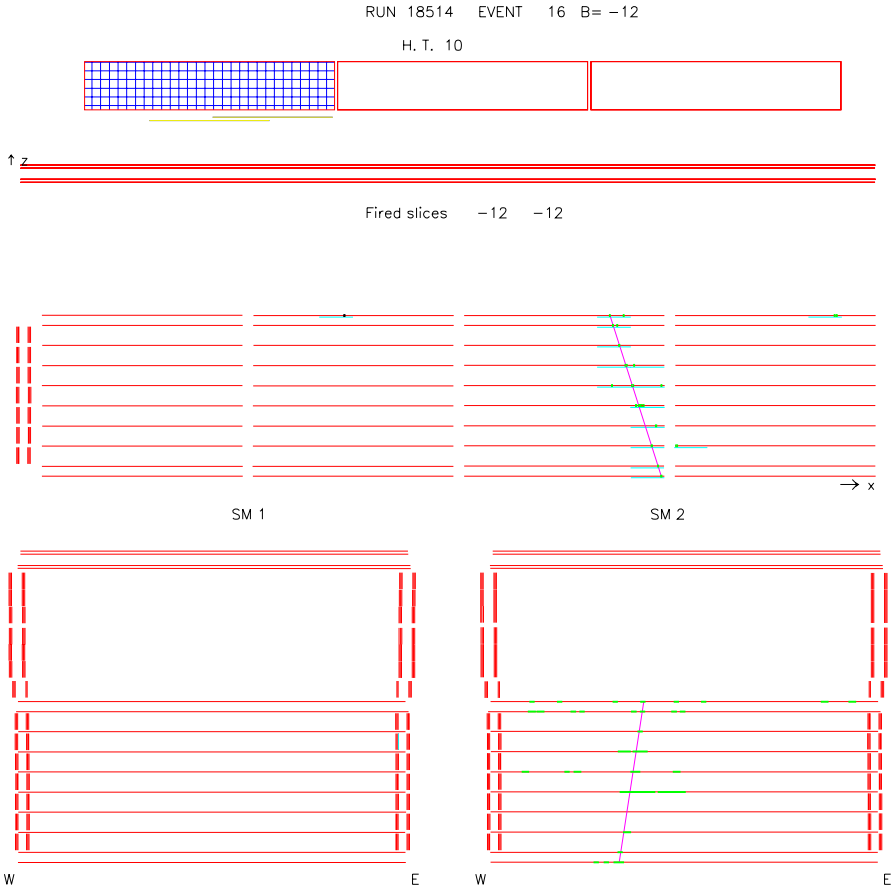

Figure 2: Space view (XZ and YZ in the upper and lower part, respectively) of a simulated catalysis event. The monopole track and the catalysis hits are clearly distinguishable.

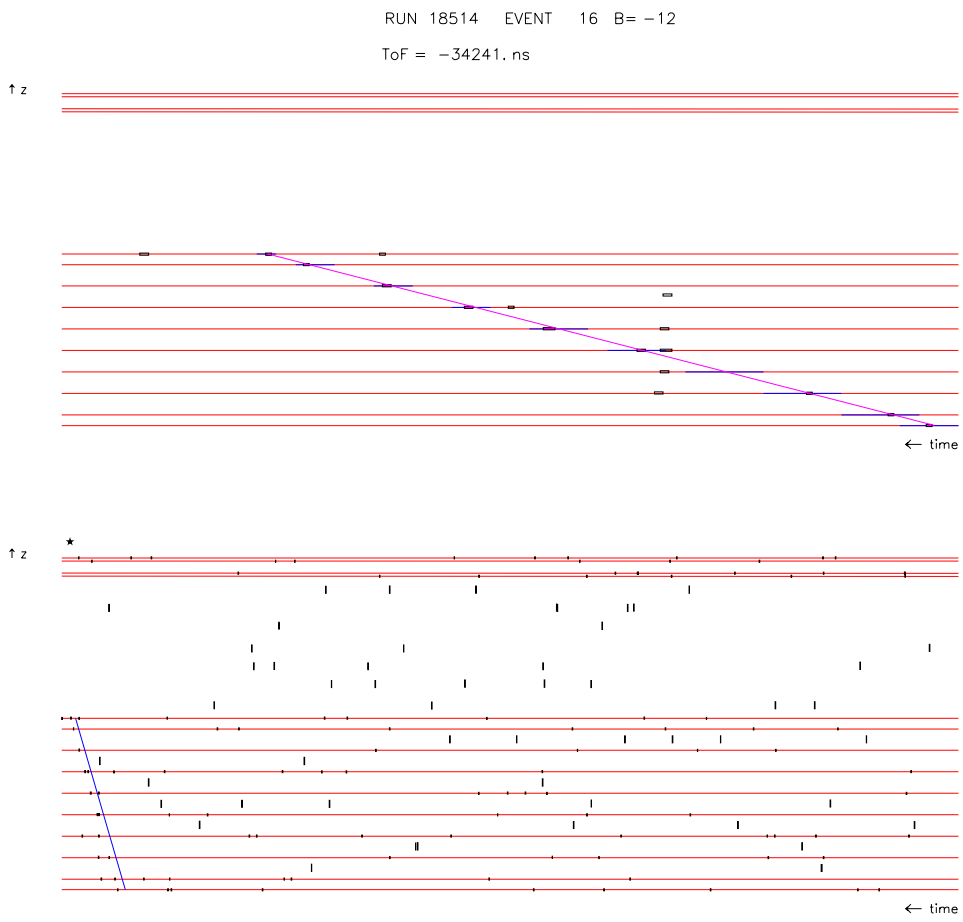

Figure 3: Time view of the simulated event shown in Fig. 2. In the lower part the content of the whole 680μs QTP memory is plotted; the upper part shows a magnification of the region around the fired β slice. The MM time track is a straight line; the catalysis hits are grouped in a narrow time window.

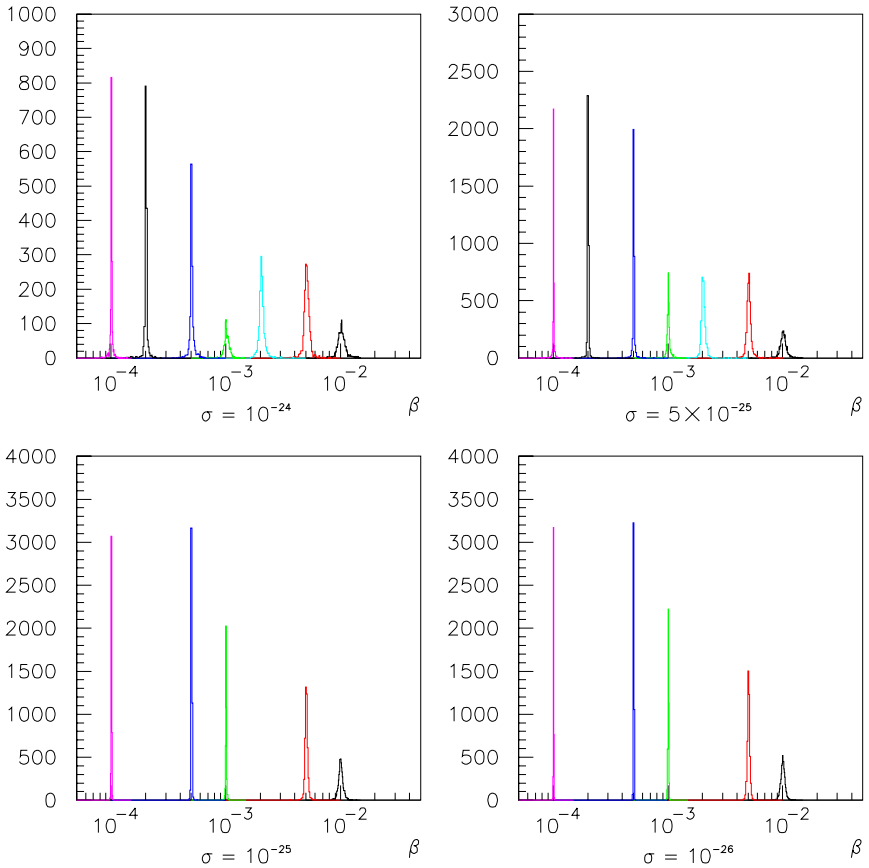

Figure 4: Distributions of the reconstructed β for 4 simulated catalysis cross sections. The distributions are exactly peaked around the input values, which means that the recontruction procedure (used in the standard streamer analysis), gives the correct β even in presence of catalysis hits.

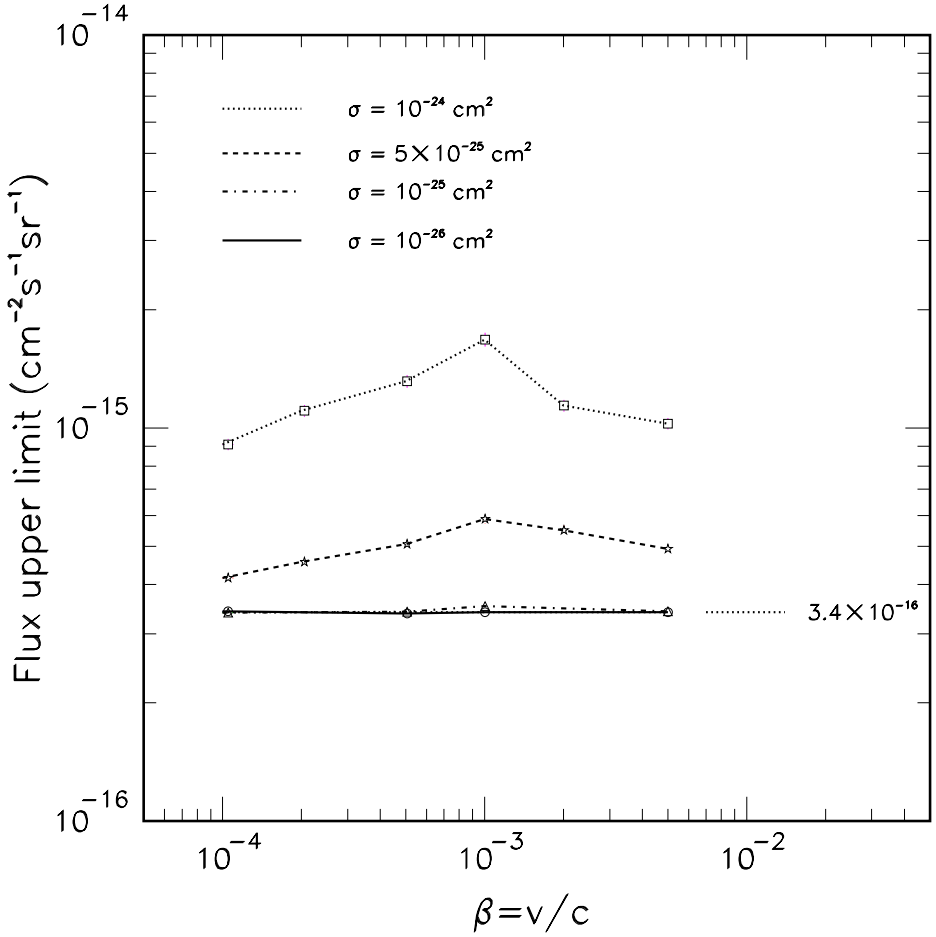

Figure 5: Flux limits from streamer tubes for 4 values of σ_{cat}, which is assumed to be the same on protons and neutrons: (from above) $\sigma_{cat} = 10^{-24}$, $5 \cdot 10^{-25}$, 10^{-25} and 10^{-26} cm^2. The simulation was performed at fixed β; the lines are only a guide to the eye.

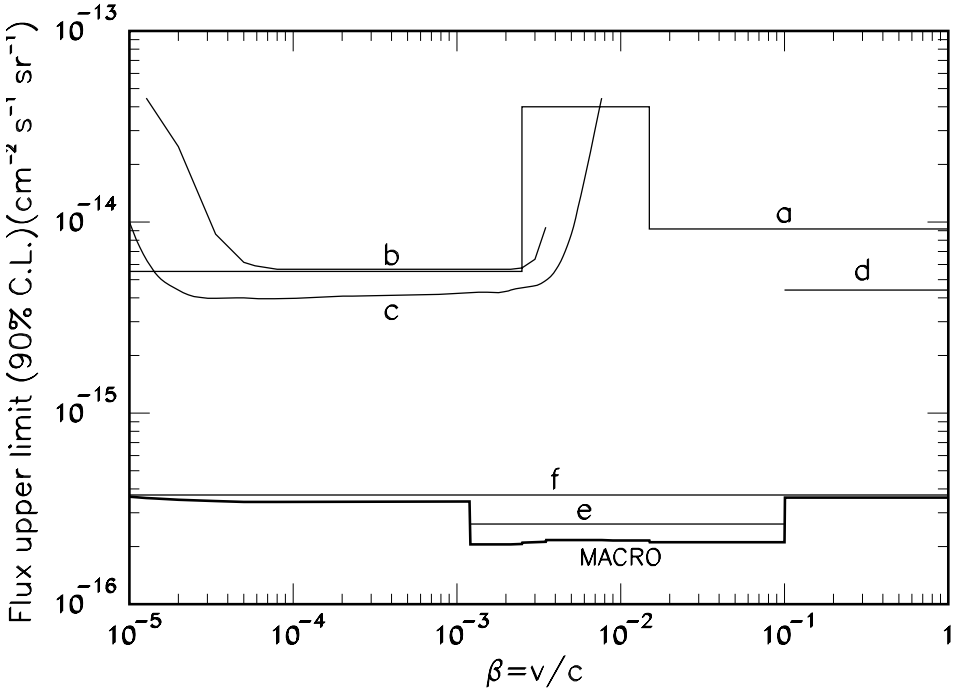

Figure 6: The 90% C.L. upper limits for an isotropic flux of nuclearites obtained using the liquid scintillator (curves "a" - "e") and the CR39 nuclear track (curve "f") subdetectors; the bold line is the MACRO global limit.

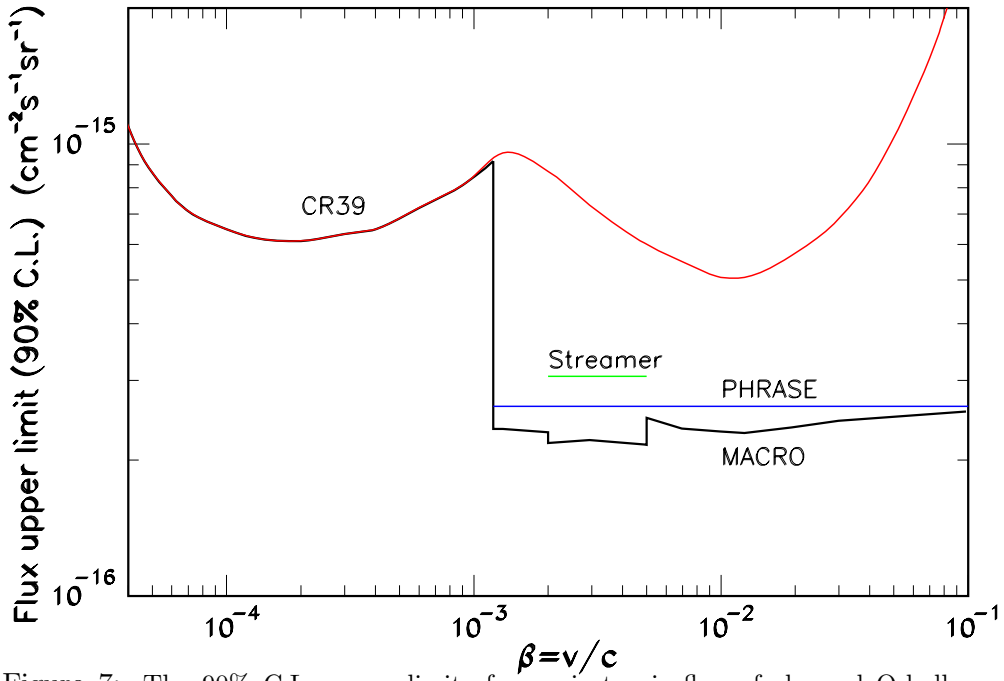

Figure 7: The 90% C.L. upper limits for an isotropic flux of charged Q-balls obtained using the liquid scintillator (curve "PHRASE"), the CR39 nuclear track detectors (curve "CR39") and the streamer tubes (curve " Streamer"). The bold line is the MACRO global limit.

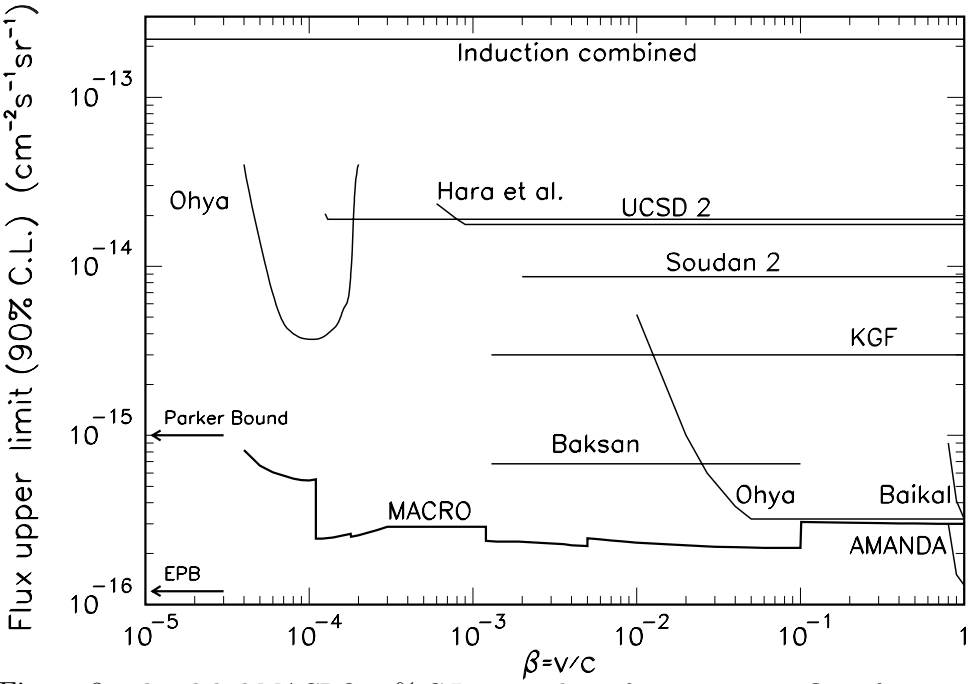

Figure 8: The global MACRO 90% C.L. upper limit for an isotropic flux of g=g_D magnetic monopoles extends from $\beta = 4 \cdot 10^{-5}$ to 1; it is compared with the limits obtained by other experiments; at values of $\beta \simeq 1$ we show the limits from the Baikal and Amanda collaborations.

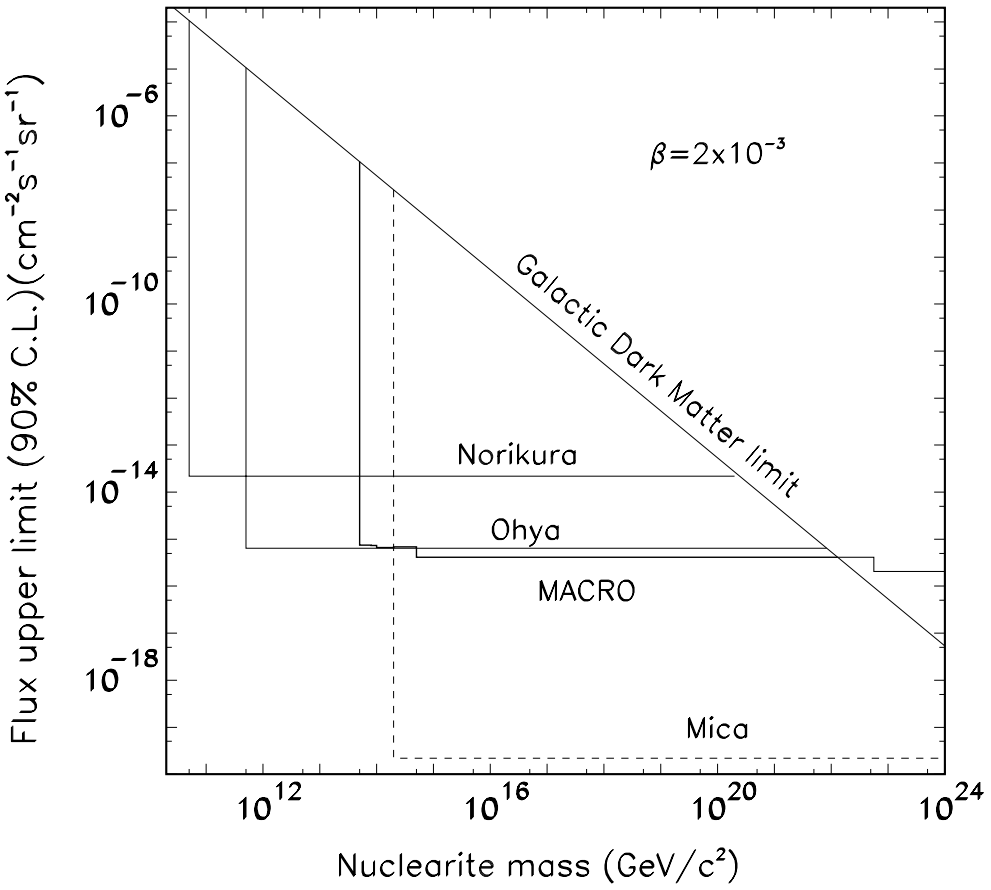

Figure 9: The global MACRO 90% C.L. upper flux limit for nuclearites with $\beta = 2 \cdot 10^{-3}$ at ground level, versus nuclearite mass, is compared with the limit obtained by other experiments and with the galactic DM bound. The limit above $M_N > 6 \cdot 10^{22}$ GeV corresponds to an isotropic flux; for $M_N < 6 \cdot 10^{22}$ GeV the limit corresponds to nuclearites reaching the detectors only from above.